MABS
2016, VOL. 8, NO. 6, 1167–1176
http://dx.doi.org/10.1080/19420862.2016.1186320

Taylor & Francis
Taylor & Francis Group

REPORT

Development and characterization of synthetic antibodies binding to the cystic fibrosis conductance regulator

Amandeep K. Gakhal[a], Timothy J. Jensen[b], Zoltan Bozoky[c,d], Ariel Roldan[e], Gergely L. Lukacs[e], Julie Forman-Kay[c,d], John R. Riordan[b], and Sachdev S. Sidhu[a]

[a]Donnelly Center for Cellular and Biomolecular Research, University of Toronto, Toronto, Ontario, Canada; [b]Department of Biochemistry and Biophysics, Cystic Fibrosis Treatment and Research Center, University of North Carolina, Chapel Hill, NC, USA; [c]Program in Molecular Structure & Function, The Hospital for Sick Children, Toronto, ON, Canada; [d]Department of Biochemistry, University of Toronto, Toronto, ON, Canada; [e]Department of Physiology and Biochemistry, McGill University, Montreal, QC, Canada

ABSTRACT

Cystic fibrosis transmembrane conductance regulator (CFTR) is a chloride channel in the apical surface of epithelial cells in the airway and gastrointestinal tract, and mutation of CFTR is the underlying cause of cystic fibrosis. However, the precise molecular details of the structure and function of CFTR in native and disease states remains elusive and cystic fibrosis researchers are hindered by a lack of high specificity, high affinity binding reagents for use in structural and biological studies. Here, we describe a panel of synthetic antigen-binding fragments (Fabs) isolated from a phage-displayed library that are specific for intracellular domains of CFTR that include the nucleotide-binding domains (NBD1 and NBD2), the R-region, and the regulatory insertion loop of NBD1. Binding assays performed under conditions that promote the native fold of the protein demonstrated that all Fabs recognized full-length CFTR. However, only the NBD1-specific Fab recognized denatured CFTR by western blot, suggesting a conformational epitope requirement for the other Fabs. Surface plasmon resonance experiments showed that the R-region Fab binds with high affinity to both the phosphorylated and unphosphorylated R-region. In addition, NMR analysis of bound versus unbound R-region revealed a distinct conformational effect upon Fab binding. We further defined residues involved with antibody recognition using an overlapping peptide array. In summary, we describe methodology complementary to previous hybridoma-based efforts to develop antibody reagents to CFTR, and introduce a synthetic antibody panel to aid structural and biological studies.

Abbreviations: ATP, adenosine triphosphate; BSA, bovine serum albumin; CDR, complementarity-determining region; CFTR, cystic fibrosis conductance regulator; DTT, dithiothreitol; ELISA, enzyme-linked immunosorbant assay; Fab, antigen-binding fragment; H_3PO_4, phosphoric acid; ICD, intracellular domain; $MgCl_2$, magnesium chloride; MSD, membrane-spanning domain; NaCl, sodium chloride; NBD, nucleotide-binding domain; NMR, nuclear magnetic resonance; PBS, phosphate-buffered saline; PKA, protein kinase A; R-region, regulatory region; RE, regulatory extension; RI, regulatory insertion; RNA, ribonucleic acid; SDS-PAGE, sodium dodecyl sulfate polyacrylamide gel electrophoresis; SPR, surface plasmon resonance

ARTICLE HISTORY
Received 3 February 2016
Revised 14 April 2016
Accepted 2 May 2016

KEYWORDS
Cystic fibrosis conductance regulator; membrane protein; phage display; protein engineering; synthetic antibody

Introduction

The cystic fibrosis transmembrane conductance regulator (CFTR) is a large multidomain protein belonging to the ABC transporter superfamily, and mutation of the CFTR gene is the underlying cause of cystic fibrosis. [1] CFTR plays an important role as an epithelial anion channel, regulating the transport of chloride ions at epithelial surfaces. The absence of functional CFTR results in disruption of ionic and water homeostasis at epithelial surfaces, interfering with normal function of the lungs, pancreas, intestines and other glandular epithelia. [2] Although high-resolution structure determination of CFTR remains elusive, insight into channel structure and function has been derived from electron microscopy studies of the full-length channel protein and NMR and X-ray crystallography studies on individual channel domains. [3-7]

As with other members of the ABC transporter family, CFTR has 2 membrane spanning domains (MSD1 and MSD2) and 2 intracellular nucleotide-binding domains (NBD1 and NBD2) (Fig. 1). [8] Extensions of the transmembrane helices into the cytoplasm form intracellular domains (ICDs) containing short coupling helices, which interact with the NBDs, and ATP binding sites are formed at the interface of the NBD heterodimer. The C-terminal end of NBD1 is also linked to MSD2 through a 200-residue region known as the regulatory (R) region, a highly dynamic, intrinsically disordered region containing multiple sites for phosphorylation by protein kinase A (PKA). [9] The N-terminal 30 residues of the R-region have been termed the regulatory extension (RE) of NBD1. An additional PKA phosphorylation site is present in the NBD1

CONTACT Sachdev S. Sidhu sachdev.sidhu@utoronto.ca
Supplemental data for this article can be accessed on the publisher's website.

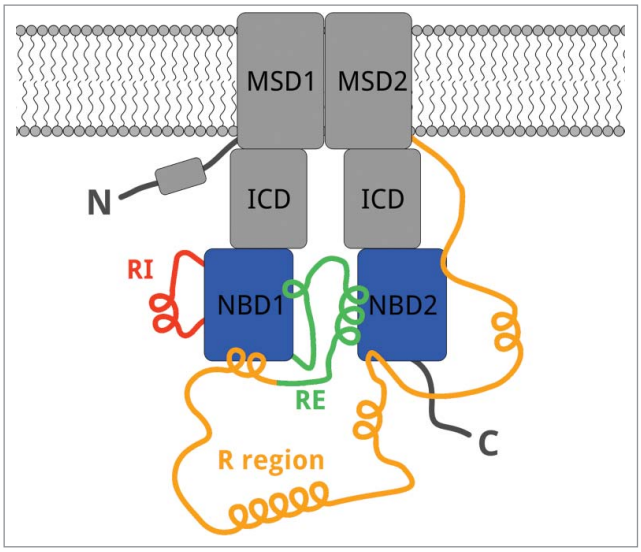

Figure 1. Structural features of CFTR. The domain organization of CFTR is illustrated as a cartoon. Membrane-spanning domains (MSD) extend to the intracellular domains (ICDs), which in turn interact with nucleotide-binding domains 1 and 2 (NBD1 and NBD2). The regulatory extension (RE) of NBD1 and phospho-regulatory elements, including the regulatory insertion (RI) of NBD1 and the regulatory region (R-region), are also highlighted.

regulatory insertion (RI), a 32-residue loop between the first 2 β strands of the domain. Together, the R-region and RI form highly dynamic phospho-regulatory elements that are hypothesized to modulate NBD interactions and structure, which in turn determine CFTR stability and regulate function. For example, NMR data indicate that a high phosphorylation state of the R-region promotes a reduced helical state that in turn reduces its interaction with NBD1 [7] and promotes channel opening. The Phe508 side-chain of NBD1 is also hypothesized to affect channel stability, and is believed to mediate critical interactions with the cytoplasmic loops of the membrane spanning domain. [8] The importance of this residue is highlighted by its deletion in the majority of cystic fibrosis patients, which results in a thermodynamically unstable protein subject to removal by quality-control mechanisms in the cell. [2,10-13] This thermal instability remains a major barrier to progress in cystic fibrosis research, and to the development of effective therapeutics.

Despite intense study, the mechanism of action of CFTR is still not fully understood. [2] Although crystal structures often provide important insights into the mechanism of action of therapeutically relevant proteins, the properties of membrane proteins such as CFTR make structural elucidation extremely difficult. [7,14] The binding of antibody fragments to membrane proteins can help overcome the problems that make membrane proteins difficult to crystallize. For example, synthetic antibody fragments have enabled high-resolution structure determination of membrane proteins, including the potassium channel protein KcsA, [15] and also large functional RNA molecules that similarly exhibit conformational flexibility. [16] However, the use of crystallization chaperones to facilitate structural studies of CFTR has been hampered by a lack of suitable antibody reagents. Although monoclonal antibodies to CFTR have been isolated, [17-19] they do not distinguish between mutant and native conformational states of CFTR. Moreover, current mouse antibodies to CFTR give weak binding signals to the channel protein in airways, where the physiological expression levels tend to be relatively low. [20,21] Importantly, assays to elucidate biological pathways and cellular function may also be hindered by a lack of high affinity reagents to probe protein function and cellular localization.

A possible explanation for this low recognition by conventional antibodies may be limitations of affinity or weak cross-reactivity to fully-native epitopes, which could potentially arise from the inability to control buffer environment during immune antigen challenge and in vivo antibody elicitation. Generation of monoclonal antibodies through mouse hybridoma technology is limited by the constraints of the immune system. In contrast, synthetic antibody technologies have emerged as a powerful method for rapid in vitro generation of high affinity recombinant antibodies. [22] Recombinant antibodies generated from in vitro selections against CFTR antigens using precisely controlled buffer conditions could potentially select antibodies with better affinities or specificity to native CFTR than has been possible with hybridoma methods.

Here, we outline approaches to systematically isolate synthetic antibodies capable of specific recognition of individual CFTR domains, describe assays for characterization of these antibodies, and report recombinant antibody fragments that will aid the cystic fibrosis research community to characterize the structure and function of CFTR.

Results

Selection of synthetic fabs binding to CFTR domains

We cycled library F, a previously described synthetic Fab-phage library, [23] through 4 rounds of binding selections against recombinant proteins representing the R-region and 2 nucleotide-binding domains (NBD1 and NBD2) of CFTR. Individual phage clones from the third and fourth selection rounds were screened for specific binding by phage ELISA. Although enrichment for specific binding Fab-phage to NBDs was low at 3%, which is likely attributable to the conformational heterogeneity of the NBDs as soluble, individual domains, specific Fabs to each domain were identified from the selections (Fig. 2b and 2d).

Five unique Fab sequences were identified for binding to the R-region and phosphorylated R-region antigens (Figs. 2a – 2c). Of the selected 30 specific binding clonal phage-Fabs sequenced, phage-Fab AB6 was observed most frequently (26/30 sequences), and phage-Fab AG6 showed the highest inhibition of ELISA binding to phosphorylated R-region when 100 nM of competing antigen was present in solution (Fig. 2c). Subsequent kinetic analysis by surface plasmon resonance (SPR) showed that Fab AG6 binds tightly to R-region antigens, with K_D values of 32 nM and 8.7 nM for R-region or phosphorylated R-region, respectively (Fig. 3).

To overcome the insolubility of NBD1, the regulatory insertion within the NBD1 domain may be deleted. Alternatively, compensating solubilizing mutations can be introduced into the full-length NBD1 protein. We examined the ability of phage-displayed Fab BB9 to bind to different NBD1 domains containing these mutations (Fig. 2d). The greatest ELISA binding signal was observed for full-length NBD1 containing 3 solubilizing mutations (NBD1 3sol), although binding signal was also observed for NBD1 domains containing

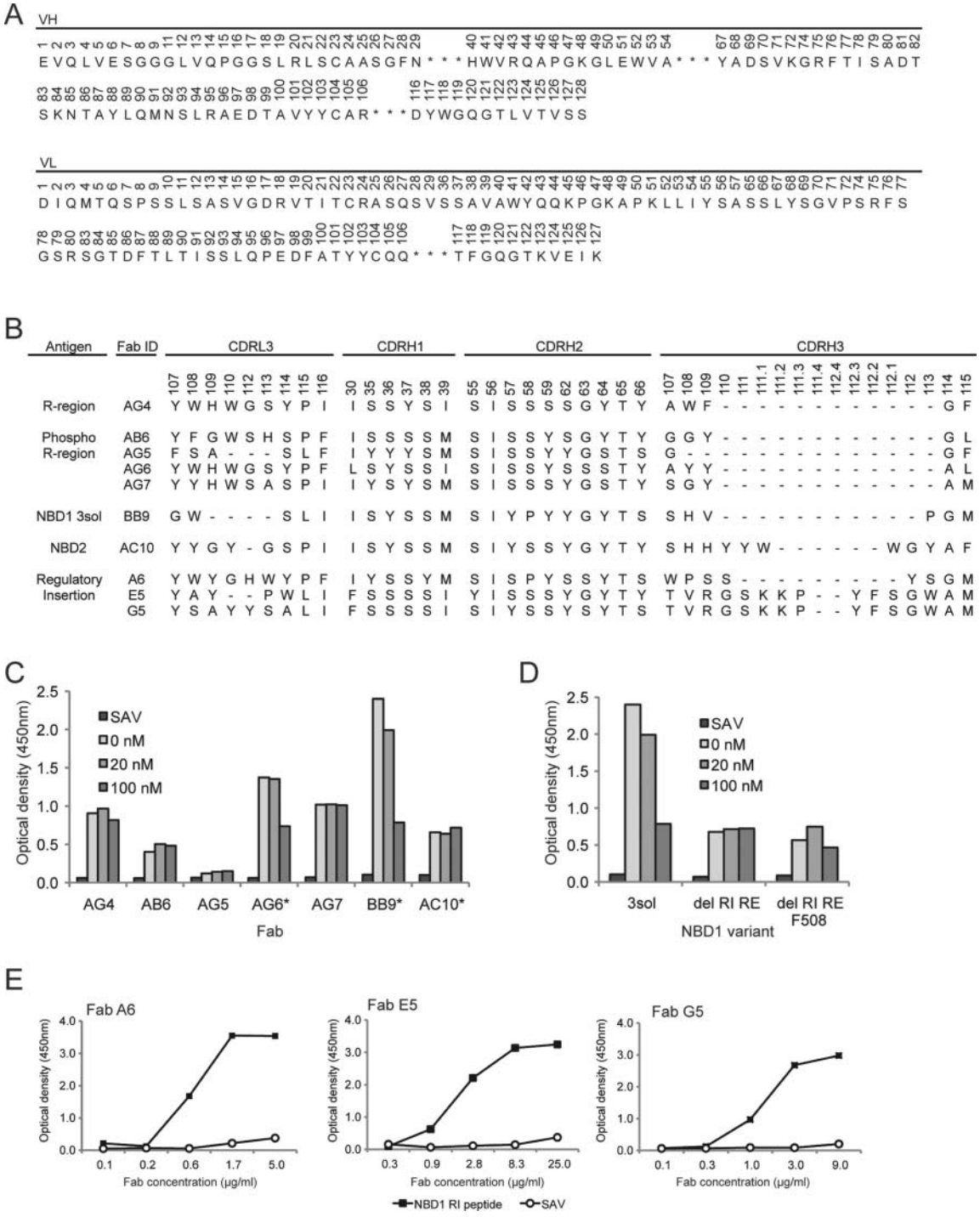

Figure 2. Fabs binding to recombinant CFTR domains. (A) Framework sequences of variable domains. VH and VL sequences are numbered according to IMGT database (http://www.imgt.org/IMGTScientificChart/Numbering/IMGT-Kabat_part1.html). Asterisks (*) indicate diversified CDR regions. (B) CDR sequences of Fabs. Positions randomized within each CDR in library F are shown at the top of each column, numbered according to IMGT standards. [37] (C) Fab-phage ELISAs for indicated Fabs binding to the CFTR domain antigens against which they were raised in the presence of the same antigens in solution at the indicated concentrations. Fabs marked with an asterisk (*) were chosen for further evaluation. (D) Fab-phage ELISAs for Fab BB9 binding to NBD1 variant containing 3 solubilizing mutations (3sol), regulatory insertion and regulatory element deletions (del RI RE), or these deletions and deletion of residue Phe508 (del RI RE F508), in the presence of the same antigens in solution at the indicated concentrations. (E) ELISAs for binding of the indicated purified Fab proteins to the biotinylated NBD1 RI peptide immobilized on SAV-coated plates (closed squares) or to SAV (open circles).

deletions of the regulatory insertion, regulatory extension, and residue F508 deletions (NBD1 del RI RE and NBD1 del RI RE F508).

We also performed binding selections against a biotinylated peptide corresponding to the regulatory insertion of NBD1 and identified 3 unique clones that bound the antigen in phage ELISAs (Fig. 2b). Two of the Fabs (E5 and G5) contained identical complementarity-determining region (CDR) H1 and H3 sequences and differed only in CDR H2 and L3, while the sequence of the third Fab (A6) was unique in all 4 CDRs that

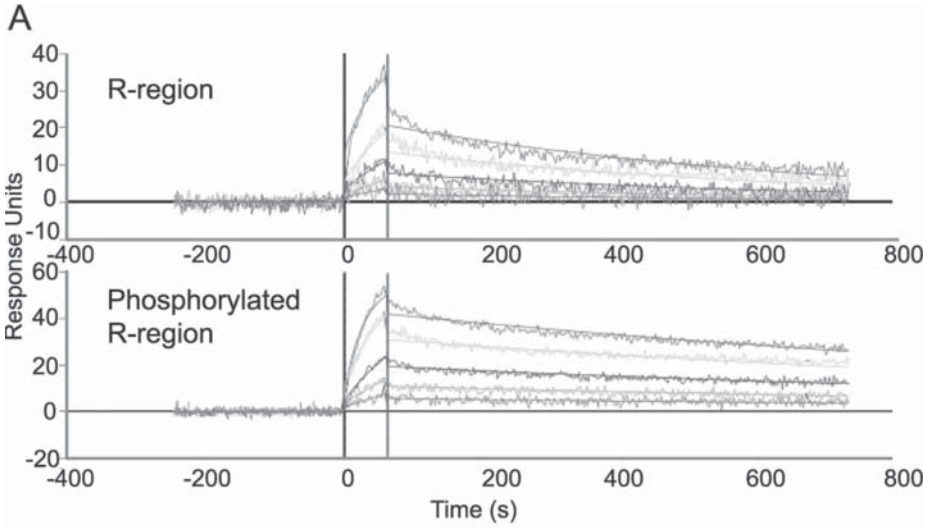

B

Antigen	k_a ($M^{-1}s^{-1}$)	k_d (s^{-1})	K_D (nM)
R-region	$5.1x10^4$	$1.6x10^{-3}$	32
Phosphorylated R-region	$8.3x10^4$	$7.2x10^{-3}$	8.7

Figure 3. Kinetic analysis of Fab AG6 binding to R-region or phosphorylated R-region. (A) SPR traces for serial dilutions of Fab AG6 binding to immobilized R-region or phosphorylated R-region. (B) Kinetic parameters (k_a and k_d) and dissociation constants (K_D) determined by globally fitting a reference cell-subtracted concentration series to a 1:1 (Langmuir) binding model. See Materials and Methods for details.

were diversified in library F. Specificity of each of the 3 Fabs for the antigen was confirmed by ELISA (Fig. 2e).

NMR analysis of fab AG6 binding to R-region and phosphorylated R-region

To examine the global effect of Fab AG6 binding to the R-region, NMR proton-nitrogen correlation (HSQC) spectra were examined for R-region and phosphorylated R-region in the absence or presence of Fab (Fig. 4a). The combined ^1H, ^{13}C and ^{15}N chemical shift changes of R-region proteins in the presence or absence of Fab AG6 (Fig. 4c and 4e) were determined, along with the intensity ratios (Fig. 4b and 4d). Based on intensity ratios, with a value of 1.0 representing no intensity change upon Fab binding, the NMR data reveal that Fab AG6 binding affects both N and C-terminal segments (residues 650–680 and 770–830) of the R-region. The dominant chemical shift changes at the R-region C-terminal segment suggest direct interactions with these

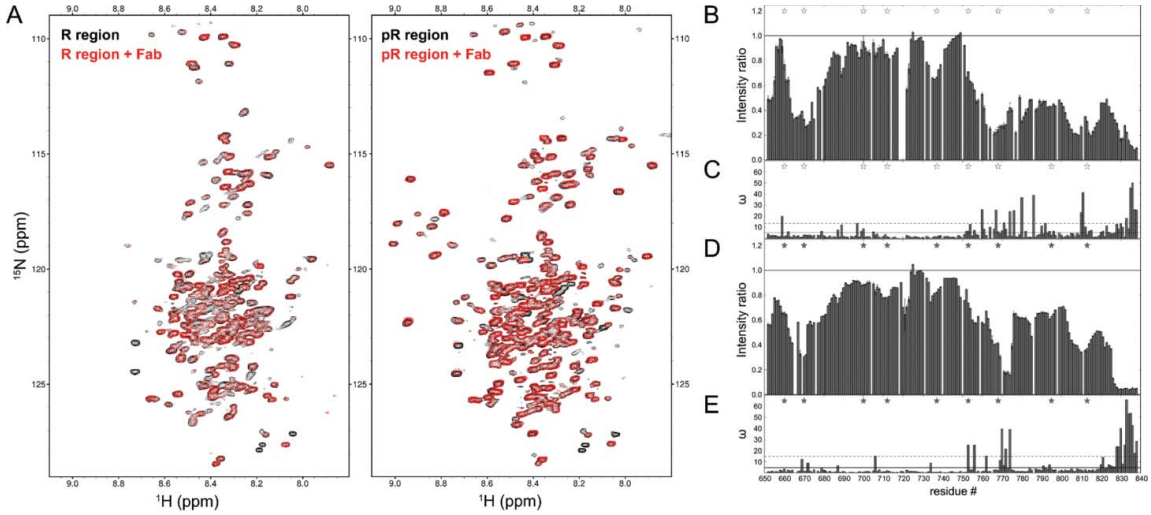

Figure 4. NMR analysis of Fab AG6 binding to R-region or phosphorylated R-region. (A) HSQC spectra of unphosphorylated (left) or phosphorylated (right) R-region in the absence (black) or presence (red) of Fab AG6. The ratio of intensity changes upon Fab AG6 binding to unphosphorylated (B) and phosphorylated R-region (D), with solid lines representing the baseline value of one, indicating no Fab binding with no change in the intensity, and error bars reflecting the propagation error from the experimental data. Combined ^1H,^{13}C and ^{15}N chemical shift changes in Hz upon Fab AG6 binding to unphosphorylated (C) or phosphorylated R-region (E), with solid lines representing the average value and dashed lines corresponding to a value plus one standard deviation from the average. In (B-E), PKA phosphorylation sites are marked as stars, open for the unphosphorylated and filled for the phosphorylated state.

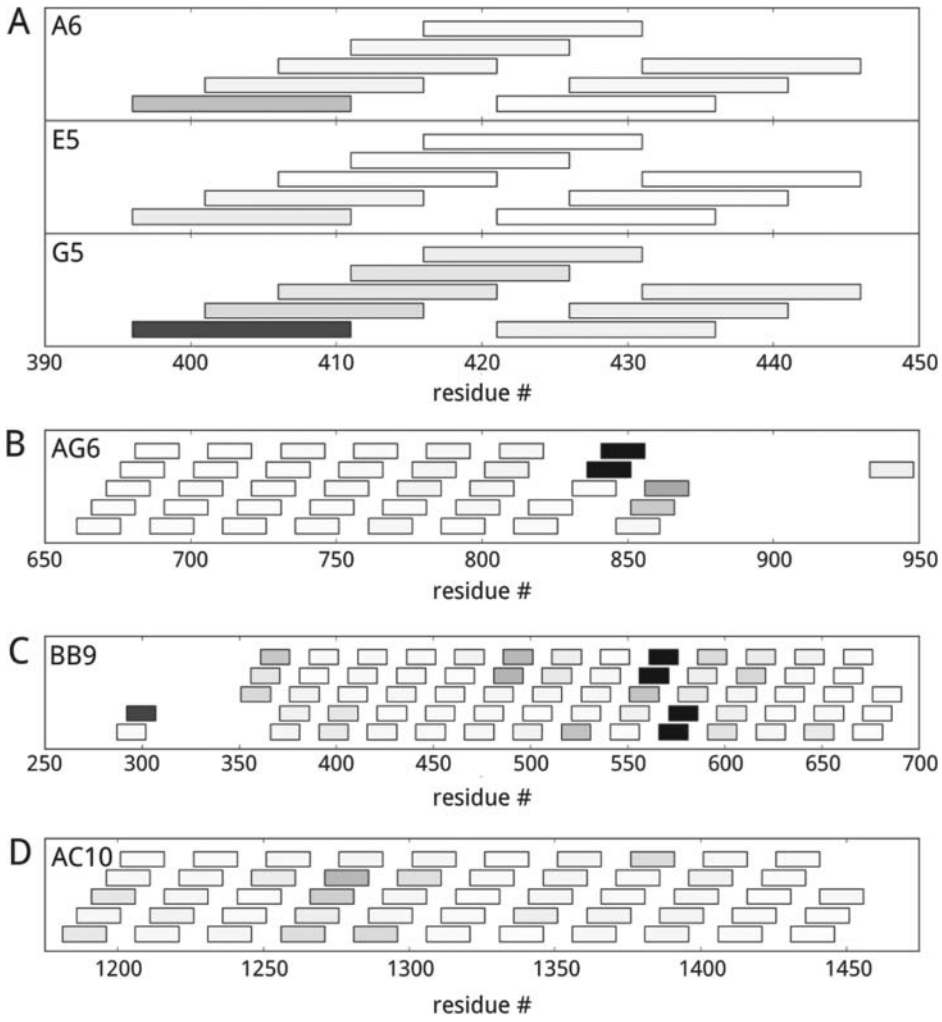

Figure 5. Binding of anti-CFTR Fabs to linear peptide arrays. Fab proteins were assayed for their ability to bind to a series of overlapping peptides representing the cytosolic sequence of CFTR. Individual peptides are represented by shaded rectangles, with black representing high binding signals and white representing low binding signals. Precise peptide boundaries and binding signals are listed in Table S1. (A) Fab A6 (top), Fab E5 (middle), and Fab G5 (bottom) were assayed for binding to overlapping peptides covering residues 396–445. (B) Fab AG6 was assayed for binding to overlapping peptides covering residues 661–947. (C) Fab BB9 was assayed for binding to overlapping peptides covering residues 287–690. (D) Fab AC10 was assayed for binding to overlapping peptides covering residues 1181–1455.

residues that lead to a stable, high-affinity complex, while other residues in the R-region likely are affected due to transient tertiary contacts with the R-region C-terminus or Fab and remain dynamic. Analysis of the direction of the amide nitrogen and carbonyl chemical shifts at the R-region C-terminus suggests moving from transient fractional helical conformations in the free state to an extended conformation in the Fab-bound states (Fig. S1). Because unphosphorylated R-region has more pronounced helical character in this segment than the phosphorylated state,[7] the chemical shift signature for this conformational change is more robust in the unphosphorylated state.

Epitope mapping of CFTR specific fabs using overlapping peptide arrays

We mapped the epitopes of the Fabs by assessing binding to a series of overlapping peptides representing the linear amino acid sequence of CFTR (Fig. 5 and Table S1). Regulatory insertion specific Fabs A6, E5, and G5, selected against N-terminally biotinylated peptide, showed only weak binding to a single peptide within the array (Fig. 5a, residues 396–410 and Table S1, peptide 44), suggesting a requirement for secondary structure within the binding epitope. In agreement with the NMR spectral changes that indicate an effect of Fab AG6 binding on C-terminal residues, we observed strong binding of Fab AG6 to 2 peptides representing the C-terminal region of CFTR (Fig. 5b, residues 836–855 and Table S1b, peptides 130 and 131). Anti-NBD1 Fab BB9 showed binding to peptides flanking residues involved in the formation of the core ATP binding region of NBD1 (Fig. 5c, residues 556–585 and Table S1c, peptides 76–79). In contrast, Fab AC10 did not show strong binding signals to overlapping peptides spanning the NBD2 domain (Fig. 5d and Table S1d).

Binding of fabs to full-length CFTR

The Fab panel was assayed for recognition of full-length CFTR protein using an ELISA performed under detergent solubilizing conditions that maintain the native fold of CFTR (Fig. 6a). In addition, full-length CFTR protein was subjected to denaturing SDS-PAGE for western blot analysis with the synthetic Fabs and a positive control mouse anti-CFTR monoclonal antibody

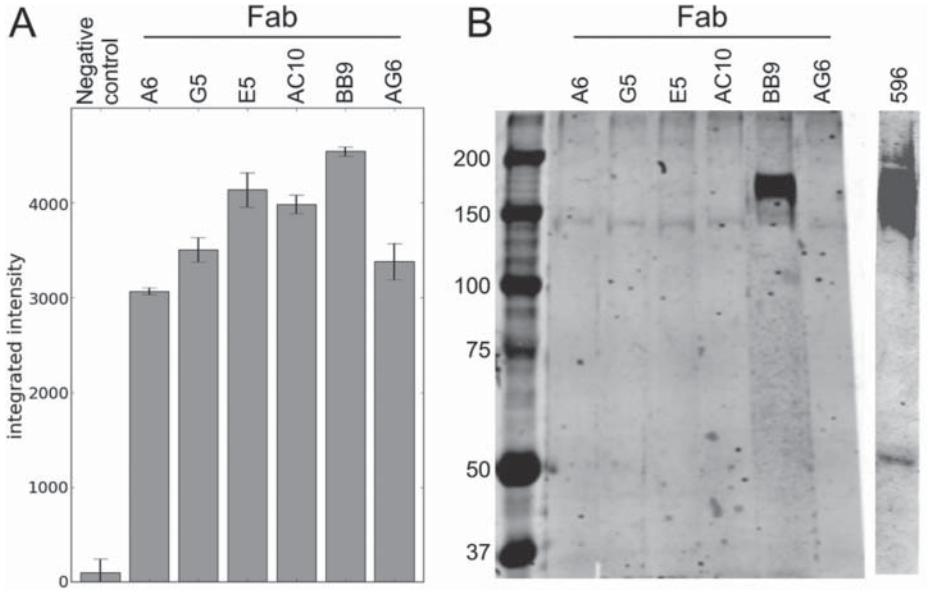

Figure 6. Fabs binding to full-length CFTR. (A) ELISAs for Fabs binding to the full-length CFTR protein under detergent conditions that maintain native folding. An anti-Her2 Fab was used as a negative control. (B) Western blots for Fabs binding to denatured full-length CFTR. An anti-CFTR mouse monoclonal antibody (596) was used as a positive control. See Materials and Methods for details.

596 (Fig. 6b). All six of the Fabs that were tested showed binding to full-length CFTR under conditions promoting channel folding, but only Fab BB9 showed binding by protein gel blot. These results indicate that Fab BB9 likely recognizes a linear epitope of NBD1 that includes residues within the peptides exhibiting binding to Fab BB9 in the overlapping peptide array (Fig. 5c). In contrast, Fab AC10 likely recognizes a conformational epitope, as supported by a lack of reactivity to linear peptides of NBD2 (Fig. 5d). Taken together with the results of our NMR studies (Fig. 4 and Fig. S1) and overlapping peptide arrays (Fig. 5b), Fab AG6 likely recognizes a complex epitope including linear regions within the R-region C-terminus (Fig. 5b Fig. S1). Upon binding to this region, Fab AG6 may induce a structural change affecting the N-terminal conformation of the protein as well (Fig. 4b). The regions or residues that form the complete Fab AG6 epitope are likely brought together within the context of the folded full-length channel protein, enabling high affinity recognition of the R-region by Fab AG6 (Fig. 3). Finally, although Fabs A6, E5 and G5 were selected against a synthetic peptide, their inability to recognize denatured CFTR in western blot analysis (Fig. 6b) and the lack of significant binding to peptides in the overlapping peptide array (Fig. 5a and Table S1a), suggests that a secondary structure within the NBD1 regulatory insertion may be required for efficient binding.

Discussion

An important advantage of in vitro phage display methods over traditional antibody hybridoma methods is the ability to tailor selection conditions to individual antigens. The CFTR channel protein contains highly mobile and disordered regions, has high dependence on a membrane environment for native structure, and has a very limited exposed external surface area.[2] These factors make preserving the native structure of CFTR during immunization very challenging and are likely central to the inability of previously isolated anti-CFTR antibodies to recognize external, discontinuous, or conformationally sensitive epitopes. However, in vitro approaches with controlled buffer conditions, such as those reported here, can enable development of antibodies capable of distinguishing conformational epitopes. We have demonstrated the application of synthetic in vitro phage-displayed antibody libraries to develop a panel of human antibodies specific for individual domains of CFTR, including NBD1, the NBD1 regulatory insertion loop, NBD2 and the R-region. We show that these Fabs can bind with high affinity to modulate structural changes upon binding (R-region specific Fab AG6) and to distinguish between unfolded (Fab BB9) and folded (Fabs AC10, AG6, E5, G5, and A6) full-length CFTR.

These antibodies are not only valuable affinity reagents that enable protein detection, but are also potentially valuable for structural studies of CFTR. The properties that make CFTR a challenging protein for antibody generation also contribute to difficulties in forming crystal contacts in high-resolution X-ray crystallography studies. However, binding of antibody fragments to both soluble and membrane protein has enabled X-ray diffracting crystals to be obtained in many cases. [15,16] More recently, Fabs have been crucial as stabilizers and symmetry determinants in single particle structure determination of proteins by cryo-electron microscopy. [24,25] Successful structural elucidation of CFTR would undoubtedly provide valuable insight into its mechanism of action and could aid drug design efforts. Moreover, given that CFTR is unique as an ABC transporter that functions as an ion channel, structural insights would also be intriguing from an evolutionary viewpoint.

The methods outlined here may also serve as an outline for future work aimed at isolating additional CFTR-specific antibodies that have proved elusive with hybridoma techniques, such as antibodies capable of distinguishing between wild-type CFTR and the ΔF508 mutant. Given that the majority of patients affected by cystic fibrosis possess the ΔF508 CFTR

mutation, high affinity reagents able to specifically detect this mutation could prove valuable in both research and clinical efforts. The F508 side-chain has been hypothesized to mediate critical interactions with the cytoplasmic loops of the membrane spanning domain, [8] and studies suggest that the ΔF508 mutation affects the biosynthetic pathway and conformational state of CFTR, such that the mutant protein is unable to pass through the endoplasmic reticulum quality control and is subsequently degraded. [2,10, 12] In addition, the ΔF508 mutant is thermodynamically unstable, and this instability contributes to the removal of mutant CFTR by quality control mechanisms in the cell [11,13, 26] and is a major challenge for therapeutic development. One method to overcome the thermal instability of mutant CFTR proteins is to employ ligands that bind with high affinity to unstable regions of the protein. Although small molecules are more typically screened as stabilizing agents, peptides and proteins can also fulfill this role with antibody binding able to stabilize mobile or disordered regions of protein antigens, [27] and antibody fragments have been used to perturb intracellular functions. [28,29] Moreover, specific in vitro selection conditions described in this work can be combined with engineering of large combinatorial protein libraries [30] to advance opportunities for tailoring antibody fragments as stabilizing intrabody agents.

Materials and methods

CFTR antigens

Human NBD1 (NBD1 del RI del RE: 387–646, Δ405–436, with and without F508del, or NBD1 3sol: 389–678, F429S, F494N, Q637R) proteins were expressed as His6-SUMO fusions at 16°C in *Escherichia coli* BL21(DE3) Codon Plus cells grown in LB media and were purified as previously described. [6,31] Three different NDB1 antigens were purified that contained either deletions of the regulatory insertion and regulatory extension regions, or residue F508 or NBD1 containing the regulatory insertion and regulatory extension with 3 solubilizing mutations introduced.

R-region and phosphorylated R-region protein domains were expressed and purified as previously described. [7]

The NBD1 regulatory insertion peptide was synthesized with an N-terminal biotin as the following amino acid sequence: Biotin-FGELFEKAKQNNNNRKTSNGDDSLFFSNF SLC-OH.

The NBD2 domain of CFTR (residues 1193–1445) contains 5 solubility mutations (Q1280E/Y1307N/H1402A/Q1411D/ L1436D) (constructed by Structural GenomiX) and was expressed as previously described [32] with changes including the use of Arctic Express DE3 RIL cells and buffers containing 20 mM sodium phosphate (pH 7.5), 100 mM Arg, and 2% (w/ v) glycine.

Fab-phage binding selections and screening

Binding selections were performed using Library F, [23] a single framework human Fab library constructed similarly to previously described libraries. [33,34] Briefly, a phagemid vector was engineered for bivalent display of a human Fab on the pIII protein of the M13 bacteriophage. All three heavy chain CDRs and the light chain CDR3 were mutagenized using oligonucleotide-directed mutagenesis with tailored mutagenic oligonucleotide mixtures. Solvent-accessible residues of CDRs H1 and H2 were restricted to tyrosine and serine residues, whereas CDRs H3 and L3 were allowed a much more complex chemical diversity of the following composition: 25% Tyr, 20% Ser, 20% Gly, 10% Ala, and 5% each of Phe, Trp, His, Pro and Val. The CDR H3 and L3 lengths were varied between 5 to 22 or 8 to 12 residues, respectively.

Library F was cycled through 4 rounds of binding selections according to modified protocols. [23] CFTR domains and phage library pools that were exposed to CFTR antigens were maintained in the following buffer conditions: NBD domains, 50 mM NaPi pH 7.0, 150 mM NaCl, 2% glycerol, 5 mM $MgCl_2$, 5 mM ATP, 5 mM DTT added immediately before use; R-region, 20 mM HEPES pH 7.5, 150 mM NaCl, 4 mM benzamidine, 2 mM DTT added immediately before use; CFTR regulatory insertion peptide, phosphate-buffered saline (PBS). Prior to resuspension of library phage for selection steps, 0.5% bovine serum albumin (BSA) was added to each solution.

Each selection round consisted of a negative selection step on 96-well Maxisorp immunoplate wells (Fisher Scientific) coated with 1% BSA in the appropriate selection buffer to remove non-specific binding Fab-phage, followed by a positive selection step on antigen-coated ELISA wells. Antigen coating was performed overnight at 4°C, phage were incubated in antigen-coated wells for 1–2 hours at 4°C, and all wash steps were performed with the appropriate selection buffer at 4°C. For peptide selections, library phage were subjected to negative selection in streptavidin- or neutravidin-coated wells and unbound phage were transferred to wells containing biotinylated peptide captured with coated streptavidin or neutravidin. Selection stringency was increased by increasing the number of wash steps with each subsequent round of selection. Bound phage were eluted from antigen-coated wells with 100 mM HCl and neutralized with 1 M Tris pH 8.0.

Selected phage pools were amplified as previously described. [35] Briefly, *E. coli* XL1blue cultures were grown to an OD_{600} of 0.8 in 2YT media containing 10 μg/ml tetracycline and infected with neutralized phage eluates. Cultures were incubated for 30 minutes at 37°C with gentle shaking and approximately 10^{10} cfu of M13 K07 helper phage were added. Cultures were incubated for 45 minutes at 37°C with shaking at 200 rpm and were transferred to 40 ml 2YT media supplemented with 100 μg/ml carbenicillin and 25 μg/ml kanamycin. Cultures were grown overnight at 37°C with shaking at 200 rpm. The amplified phage pool was harvested for subsequent selection rounds as described. [35]

Antigen-binding Fab-phage were identified by clonal phage ELISAs. Clonal bacterial cultures harboring phagemid were grown overnight at 37°C in 96-well deep well plates with 2YT media containing 100 μg/ml carbenicillin and 10^{10} cfu/ml of M13 K07 helper phage. Phage ELISAs were performed using antigen coating, blocking, and phage incubation conditions similar to those used during binding selections. After washing, anti-M13-HRP (GE Healthcare, Piscataway, NJ) was diluted in appropriate buffer (DTT was omitted during this step) and allowed to bind for 45–60 minutes at 4°C. Plates were washed

and bound phage were detected using 3,3′,5,5′-tetramethylbenzidine substrate (Sigma-Aldrich, St. Louis, MO). The reactions were quenched using equal volumes of 0.5 M sulfuric acid, and the absorbance at 450 nm was measured.

Protein expression and purification

Fab proteins were purified from *E. coli* 55244 cultures harboring phagemids modified by the insertion of an amber stop codon between the Fab and pIII proteins to facilitate secretion of free Fab protein. [35] Clonal cultures were grown overnight at 30°C in 2YT media supplemented with 50 μg/ml carbenicillin and 25 μg/ml kanamycin. Cultures were centrifuged at 3000 g for 10 minutes and pellets were re-suspended in 25 ml of a phosphate limiting media, complete CRAP media,[35] that supports induction of the phoA promoter. Ten ml re-suspended culture was used to inoculate 1 L CRAP media, which was incubated for 24 hours at 30°C, pelleted, re-suspended in 25 ml PBS, and frozen. Pellets were thawed, resuspended in 30 ml lysis buffer (50 mM Tris-HCl, 150 mM NaCl, pH 8.0) containing 15 mg lysozyme (Bioshop) and 30 μl DNase I (deoxyribonuclease I, Fermentus)) and lysed by sonication. Following centrifugation to pellet cell debris, supernatants were loaded onto fast-flow rProtein A-Sepharose (GE Healthcare) pre-equilibrated in PBS. Columns were washed with PBS, eluted with 50 mM NaH_2PO_4, 100 mM H_3PO_4, 140 mM NaCl, pH 2.5. Eluates were neutralized with 1 M Na_2HPO_4, 140 mM NaCl and buffer exchanged into desired buffers using Amicon 10K MWCO centrifugal filters. Purified Fab proteins were analyzed by SDS-PAGE and quantified using a Bradford assay (Bio-Rad) or the absorbance at A280 using an IgG conversion factor.

NMR and R-region interaction experiments

NMR measurements were collected on a Varian Inova 800-MHz spectrometer at 10°C with a triple-resonance probe. Recorded data were processed using NMRPipe [36] and analyzed using Sparky (http://www.cgl.ucsf.edu/home/sparky/). Complete phosphorylation was achieved by incubation with PKA (NEB: P6000S), and was monitored by mass spectrometry and NMR spectroscopy.[7] HNCO spectra were recorded with 8 transients at 10°C with 150 μM $^{15}N^{13}C$ R-region samples in the absence or presence of 200 μM Fab (1.33x molar excess) in 50 mM NaH_2PO_4 pH 7.20; 100 mM NaCl; 2 mM DTT; 10% (v/v) D_2O.

Surface plasmon resonance

The kinetic parameters for interactions between Fabs and CFTR domains were measured by SPR using a ProteOn XPR36 instrument (Bio-Rad). Antigens were immobilized on a GLC chip by amine coupling chemistry and serial dilutions of Fab in PBS with 0.05% Tween 20 were injected over the antigen and blank channels (for reference subtraction) for 60 seconds at a flow rate of 100 μl/min, followed by 10 minutes of buffer to monitor Fab dissociation. The chip surface was regenerated with 0.85% H_3PO_4 prior to new analyte injection. Kinetic parameters were determined by globally fitting a reference cell-subtracted concentration series to a 1:1 (Langmuir) binding model.

Epitope mapping of anti-CFTR fabs

An overlapping peptide array spanning the predicted cytosolic regions of the human CFTR was used to identify the anti-CFTR Fab epitopes. The array consisted of 15-residue peptides with 5 residues offset and a covalently attached biotin tag at the N-terminus, synthesized by Mimotopes, The Peptide Company. Unless otherwise stated, all binding steps were performed in PBS containing 0.05% Tween 20, pH 7.4 (PBS/T) at room temperature and 3 washes with PBS/T between binding steps. For the ELISA, approximately 10 picomoles peptide was captured onto 96-well Streptavidin plates (Nunc) for one hour. Plates were blocked with 0.5% BSA in PBS/T for 0.5 hour and Fabs were bound in PBS/T supplemented with 1% BSA for one hour, followed by binding of horseradish peroxidase (HRP)-conjugated anti-flag M2 antibody (Sigma) in PBS/T, 1% BSA for one hour. The fluorescence generated by HRP in the presence of 60 mM Amplex-Red was measured, using a fluorescence plate reader at 560 nm excitation and 590 nm emission wavelength. Background fluorescence was determined in the absence of peptide.

Full- length CFTR ELISA

His-Grab Nickel coated plates (Pierce) were coated with 75 ng/well of Deca-His-tagged CFTR in PBS, 0.1% DDM overnight at 4°C. Wells were blocked for 1 hour with PBS, 1% BSA, 5% normal goat serum (blocking buffer). Fifty ml Fab stocks (10 μg/ml) in blocking buffer were added to wells in quadruplicates and incubated for 2 hours. Wells were washed with PBS and mouse anti-human kappa secondary antibody was added and incubated for 1 hour. After washing, goat anti-mouse fluorescent antibody was added for 1 hour. Plates were washed with PBS and scanned using Fuji FLA-5100 scanner. TIFF images were quantified using ImageJ.

Western Blotting

Western blots were performed as described. [18] Briefly, 75 μg crude membranes prepared from BHK cells expressing CFTR were run on a 7% gel and transferred to nitrocellulose. Nitrocellulose was blocked using 5% Carnation powdered milk in PBS. Fab protein (10 μg/ml) in blocking buffer was added and incubated for 2 hours. Blots were washed with PBS between each antibody application. Mouse anti-human kappa was added for 1 hour followed by fluorescently tagged goat anti-mouse antibody. Blots were scanned using a Li-Cor Odyssey fluorescent scanner.

Disclosure of potential conflicts of interest

No potential conflicts of interest were disclosed.

Acknowledgments

We acknowledge Drs. Rhea Hudson and Jennifer Dawson for preparation of NBD1 and NBD2 protein samples.

Funding

This study was supported by CIHR grant MOP-136944 (S.S.S.) and by grants from Cystic Fibrosis Canada (J.D.F.-K. and G.L.L.), Cystic Fibrosis

Foundation Therapeutics (J.D.F.-K.), NIH RO1DK051870 (to J.R.R.) and CIHR and NIH-NIDDK (G.L.L.). 8 A. K. GAKHAL ET AL. Fellowship support was provided by Cystic Fibrosis Canada (A.K.G). G.L.L. is recipient of a Canada Research Chair.

References

1. Riordan JR, Rommens JM, Kerem B, Alon N, Rozmahel R, Grzelczak Z, Zielenski J, Lok S, Plavsic N, Chou JL. Identification of the cystic fibrosis gene: cloning and characterization of complementary DNA. Science 1989; 245:1066-73; PMID:2475911; http://dx.doi.org/10.1126/science.2475911
2. Riordan JR. CFTR function and prospects for therapy. Annu Rev Biochem 2008; 77:701-26; PMID:18304008; http://dx.doi.org/10.1146/annurev.biochem.75.103004.142532
3. Lewis HA, Buchanan SG, Burley SK, Conners K, Dickey M, Dorwart M, Fowler R, Gao X, Guggino WB, Hendrickson WA, et al. Structure of nucleotide-binding domain 1 of the cystic fibrosis transmembrane conductance regulator. EMBO J 2004; 23:282-93; PMID:14685259; http://dx.doi.org/10.1038/sj.emboj.7600040
4. Thibodeau PH, Brautigam CA, Machius M, Thomas PJ. Side chain and backbone contributions of Phe508 to CFTR folding. Nat Struct Mol Biol 2005; 12:10-6; PMID:15619636; http://dx.doi.org/10.1038/nsmb881
5. Zhang L, Aleksandrov LA, Zhao Z, Birtley JR, Riordan JR, Ford RC. Architecture of the cystic fibrosis transmembrane conductance regulator protein and structural changes associated with phosphorylation and nucleotide binding. J Struct Biol 2009; 167:242-51; PMID:19524678; http://dx.doi.org/10.1016/j.jsb.2009.06.004
6. Kanelis V, Hudson RP, Thibodeau PH, Thomas PJ, Forman-Kay JD. NMR evidence for differential phosphorylation-dependent interactions in WT and DeltaF508 CFTR. EMBO J 2010; 29:263-77; PMID:19927121; http://dx.doi.org/10.1038/emboj.2009.329
7. Baker JM, Hudson RP, Kanelis V, Choy WY, Thibodeau PH, Thomas PJ, Forman-Kay JD. CFTR regulatory region interacts with NBD1 predominantly via multiple transient helices. Nat Struct Mol Biol 2007; 14:738-45; PMID:17660831; http://dx.doi.org/10.1038/nsmb1278
8. Serohijos AW, Hegedus T, Aleksandrov AA, He L, Cui L, Dokholyan NV, Riordan JR. Phenylalanine-508 mediates a cytoplasmic-membrane domain contact in the CFTR 3D structure crucial to assembly and channel function. Proc Natl Acad Sci U S A 2008; 105:3256-61; PMID:18305154; http://dx.doi.org/10.1073/pnas.0800254105
9. Ostedgaard LS, Baldursson O, Vermeer DW, Welsh MJ, Robertson AD. A functional R domain from cystic fibrosis transmembrane conductance regulator is predominantly unstructured in solution. Proc Natl Acad Sci U S A 2000; 97:5657-62; PMID:10792060; http://dx.doi.org/10.1073/pnas.100588797
10. Cheng SH, Rich DP, Marshall J, Gregory RJ, Welsh MJ, Smith AE. Phosphorylation of the R domain by cAMP-dependent protein kinase regulates the CFTR chloride channel. Cell 1991; 66:1027-36; PMID:1716180; http://dx.doi.org/10.1016/0092-8674(91)90446-6
11. Hegedus T, Aleksandrov A, Cui L, Gentzsch M, Chang XB, Riordan JR. F508del CFTR with two altered RXR motifs escapes from ER quality control but its channel activity is thermally sensitive. Biochim Biophys Acta 2006; 1758:565-72; PMID:16624253; http://dx.doi.org/10.1016/j.bbamem.2006.03.006
12. Kopito RR. Biosynthesis and degradation of CFTR. Physiol Rev 1999; 79:S167-73; PMID:9922380
13. Sharma M, Benharouga M, Hu W, Lukacs GL. Conformational and temperature-sensitive stability defects of the delta F508 cystic fibrosis transmembrane conductance regulator in post-endoplasmic reticulum compartments. J Biol Chem 2001; 276:8942-50; PMID:11124952; http://dx.doi.org/10.1074/jbc.M009172200
14. Hegedus T, Serohijos AW, Dokholyan NV, He L, Riordan JR. Computational studies reveal phosphorylation-dependent changes in the unstructured R domain of CFTR. J Mol Biol 2008; 378:1052-63; PMID:18423665; http://dx.doi.org/10.1016/j.jmb.2008.03.033
15. Uysal S, Vasquez V, Tereshko V, Esaki K, Fellouse FA, Sidhu SS, Koide S, Perozo E, Kossiakoff A. Crystal structure of full-length KcsA in its closed conformation. Proc Natl Acad Sci U S A 2009; 106:6644-9; PMID:19346472; http://dx.doi.org/10.1073/pnas.0810663106
16. Ye JD, Tereshko V, Frederiksen JK, Koide A, Fellouse FA, Sidhu SS, Koide S, Kossiakoff AA, Piccirilli JA. Synthetic antibodies for specific recognition and crystallization of structured RNA. Proc Natl Acad Sci U S A 2008; 105:82-7; PMID:18162543; http://dx.doi.org/10.1073/pnas.0709082105
17. Cohn JA, Melhus O, Page LJ, Dittrich KL, Vigna SR. CFTR: development of high- affinity antibodies and localization in sweat gland. Biochem Biophys Res Commun 1991; 181:36-43; PMID:1720311; http://dx.doi.org/10.1016/S0006-291X(05)81378-6
18. Cui L, Aleksandrov L, Chang XB, Hou YX, He L, Hegedus T, Gentzsch M, Aleksandrov A, Balch WE, Riordan JR. Domain interdependence in the biosynthetic assembly of CFTR. J Mol Biol 2007; 365:981-94; PMID:17113596; http://dx.doi.org/10.1016/j.jmb.2006.10.086
19. Kartner N, Hanrahan JW, Jensen TJ, Naismith AL, Sun SZ, Ackerley CA, Reyes EF, Tsui LC, Rommens JM, Bear CE. Expression of the cystic fibrosis gene in non-epithelial invertebrate cells produces a regulated anion conductance. Cell 1991; 64:681-91; PMID:1705179; http://dx.doi.org/10.1016/0092-8674(91)90498-N
20. Kreda SM, Mall M, Mengos A, Rochelle L, Yankaskas J, Riordan JR, Boucher RC. Characterization of wild-type and deltaF508 cystic fibrosis transmembrane regulator in human respiratory epithelia. Mol Biol Cell 2005; 16:2154-67; PMID:15716351; http://dx.doi.org/10.1091/mbc.E04-11-1010
21. Mall M, Kreda SM, Mengos A, Jensen TJ, Hirtz S, Seydewitz HH, Yankaskas J, Kunzelmann K, Riordan JR, Boucher RC. The DeltaF508 mutation results in loss of CFTR function and mature protein in native human colon. Gastroenterology 2004; 126:32-41; PMID:14699484; http://dx.doi.org/10.1053/j.gastro.2003.10.049
22. Adams JJ, Sidhu SS. Synthetic antibody technologies. Curr Opin Struct Biol 2014; 24:1-9; PMID:24721448; http://dx.doi.org/10.1016/j.sbi.2013.11.003
23. Persson H, Ye W, Wernimont A, Adams JJ, Koide A, Koide S, Lam R, Sidhu SS. CDR-H3 Diversity Is Not Required for Antigen Recognition by Synthetic Antibodies. J Mol Biol 2012; 425:803-11; PMID:23219464; http://dx.doi.org/10.1016/j.jmb.2012.11.037
24. Kim J, Wu S, Tomasiak TM, Mergel C, Winter MB, Stiller SB, Robles-Colmanares Y, Stroud RM, Tampé R, Craik CS, et al. Subnanometre-resolution electron cryomicroscopy structure of a heterodimeric ABC exporter. Nature 2015; 517:396-400; PMID:25363761; http://dx.doi.org/10.1038/nature13872
25. Wu S, Avila-Sakar A, Kim J, Booth DS, Greenberg CH, Rossi A, Liao M, Li X, Alian A, Griner SL, et al. Fabs enable single particle cryoEM studies of small proteins. Structure 2012; 20:582-92; PMID:22483106; http://dx.doi.org/10.1016/j.str.2012.02.017
26. Okiyoneda T, Barriere H, Bagdany M, Rabeh WM, Du K, Hohfeld J, Young JC, Lukacs GL. Peripheral protein quality control removes unfolded CFTR from the plasma membrane. Science 2010; 329:805-10; PMID:20595578; http://dx.doi.org/10.1126/science.1191542
27. Michnick SW, Sidhu SS. Submitting antibodies to binding arbitration. Nat Chem Biol 2008; 4:326-9; PMID:18488004; http://dx.doi.org/10.1038/nchembio0608-326
28. Newnham LE, Wright MJ, Holdsworth G, Kostarelos K, Robinson MK, Rabbitts TH, Lawson AD. Functional inhibition of beta-catenin-mediated Wnt signaling by intracellular VHH antibodies. MAbs 2015; 7:180-91; PMID:25524068; http://dx.doi.org/10.4161/19420862.2015.989023
29. Colby DW, Chu Y, Cassady JP, Duennwald M, Zazulak H, Webster JM, Messer A, Lindquist S, Ingram VM, Wittrup KD. Potent inhibition of huntingtin aggregation and cytotoxicity by a disulfide bond-free single-domain intracellular antibody. Proc Natl Acad Sci U S A 2004; 101:17616-21; PMID:15598740; http://dx.doi.org/10.1073/pnas.0408134101
30. Gilbreth RN, Esaki K, Koide A, Sidhu SS, Koide S. A dominant conformational role for amino acid diversity in minimalist protein-protein interfaces. J Mol Biol 2008; 381:407-18; PMID:18602117; http://dx.doi.org/10.1016/j.jmb.2008.06.014
31. Lewis HA, Zhao X, Wang C, Sauder JM, Rooney I, Noland BW, Lorimer D, Kearins MC, Conners K, Condon B, et al. Impact of the deltaF508 mutation in first nucleotide-binding domain of human cystic fibrosis transmembrane conductance regulator on domain folding and structure. J Biol Chem 2005; 280:1346-53; PMID:15528182; http://dx.doi.org/10.1074/jbc.M410968200

32. Bozoky Z, Krzeminski M, Muhandiram R, Birtley JR, Al-Zahrani A, Thomas PJ, Frizzell RA, Ford RC, Forman-Kay JD. Regulatory R region of the CFTR chloride channel is a dynamic integrator of phospho-dependent intra- and intermolecular interactions. Proc Natl Acad Sci U S A 2013; 110: E4427-36; PMID:24191035; http://dx.doi.org/10.1073/pnas.1315104110
33. Fellouse FA, Esaki K, Birtalan S, Raptis D, Cancasci VJ, Koide A, Jhurani P, Vasser M, Wiesmann C, Kossiakoff AA, et al. High-throughput generation of synthetic antibodies from highly functional minimalist phage-displayed libraries. J Mol Biol 2007; 373:924-40; PMID:17825836; http://dx.doi.org/10.1016/j.jmb.2007.08.005
34. Fellouse FA, Pal G. Methods for the Construction of Phage-Displayed Libraries. In: Sidhu SS, ed. Phage Display in Biotechnology and Drug Discovery. Boca Raton: CRC Press, 2005.
35. Tonikian R, Zhang Y, Boone C, Sidhu SS. Identifying specificity profiles for peptide recognition modules from phage-displayed peptide libraries. Nat Protoc 2007; 2:1368-86; PMID:17545975; http://dx.doi.org/10.1038/nprot.2007.151
36. Delaglio F, Grzesiek S, Vuister GW, Zhu G, Pfeifer J, Bax A. NMRPipe: a multidimensional spectral processing system based on UNIX pipes. J Biomol NMR 1995; 6:277-93; PMID:8520220; http://dx.doi.org/10.1007/BF00197809
37. Lefranc MP, Pommie C, Ruiz M, Giudicelli V, Foulquier E, Truong L, Thouvenin-Contet V, Lefranc G. IMGT unique numbering for immunoglobulin and T cell receptor variable domains and Ig superfamily V-like domains. Dev Comp Immunol 2003; 27:55-77; PMID:12477501; http://dx.doi.org/10.1016/S0145-305X(02)00039-3